

# JAX-Accelerated Neuroevolution of Physics-informed Neural Networks: Benchmarks and Experimental Results

Nicholas Sung Wei Yong<sup>a,1</sup>, Jian Cheng Wong<sup>a,b</sup>, Pao-Hsiung Chiu<sup>a</sup>, Abhishek Gupta<sup>a,b</sup>, Chinchun Ooi<sup>a</sup>, Yew-Soon Ong<sup>a,b</sup>

<sup>a</sup> Agency for Science, Technology and Research (A\*STAR), 138632, Singapore

<sup>b</sup> School of Computer Science and Engineering, Nanyang Technological University, 639798, Singapore

---

**Abstract** – This paper introduces the use of evolutionary algorithms for solving differential equations. The solution is obtained by optimizing a deep neural network whose loss function is defined by the residual terms from the differential equations. Recent studies have used stochastic gradient descent (SGD) variants to train these physics-informed neural networks (PINNs), but these methods can struggle to find accurate solutions due to optimization challenges. When solving differential equations, it is important to find the globally optimum parameters of the network, rather than just finding a solution that works well during training. SGD only searches along a single gradient direction, so it may not be the best approach for training PINNs with their accompanying complex optimization landscapes. In contrast, evolutionary algorithms perform a parallel exploration of different solutions in order to avoid getting stuck in local optima and can potentially find more accurate solutions. However, evolutionary algorithms can be slow, which can make them difficult to use in practice. To address this, we provide a set of five benchmark problems with associated performance metrics and baseline results to support the development of evolutionary algorithms for enhanced PINN training. As a baseline, we evaluate the performance and speed of using the widely adopted Covariance Matrix Adaptation Evolution Strategy (CMA-ES) for solving PINNs. We provide the loss and training time for CMA-ES run on TensorFlow (both with and without GPU acceleration), and CMA-ES and SGD run on JAX (with GPU acceleration) for the five benchmark problems. Our results show that JAX-accelerated evolutionary algorithms, particularly CMA-ES, can be a useful approach for solving differential equations. We hope that our work will support the exploration and development of alternative optimization algorithms for the complex task of optimizing PINNs.

---

## 1. Introduction

Physics-informed neural networks (PINNs) are a type of deep learning model that incorporates physical laws and constraints into the training process. PINNs combine the expressive power of neural networks with the guarantees accorded by compliance with physical laws and principles. This allows PINNs to make predictions that are not only accurate, but also physically meaningful and consistent with known laws of nature.

In the current literature [1], PINNs are typically trained by using a combination of data and physical constraints. In essence, a PINN model incorporates the governing physics of the dynamical process as a known prior into the loss function. It uses the weighted sum of the residual terms from the differential equation ( $\mathcal{L}_{PDE}$ ), and the prescribed initial ( $\mathcal{L}_{IC}$ ) and/or boundary ( $\mathcal{L}_{BC}$ ) conditions as the loss function ( $\mathcal{L}_{Physics}$ ) which is defined below:

$$\mathcal{L}_{Physics} = \lambda_{PDE}\mathcal{L}_{PDE} + \lambda_{IC}\mathcal{L}_{IC} + \lambda_{BC}\mathcal{L}_{BC} \quad (1)$$

The neural network framework is able to learn from the data, while the physical constraints are used to regularize the learning process and ensure that the predictions of the network remain consistent with known physical laws and constraints. This allows PINNs to generalize better and make accurate predictions even on test-time data. The

---

<sup>1</sup> Corresponding author.

Email address: nicholas\_sung@cfar.a-star.edu.sg (Nicholas Sung Wei Yong)

utility of this framework has been demonstrated on various complex scientific and engineering problems, towards purposes such as predicting the behaviour of physical systems, modelling the properties of materials, and assimilating data from experiments and simulations [2].

While promising and very effective when successfully learned, PINN training has been shown to be complex, and prone to various failure mechanisms even when state-of-the-art stochastic gradient descent-based methods are used for training [3]. A variety of challenges have been identified in previous work, especially when local optimization methods like gradient descent algorithms are used. These include the need for proper balancing of the competing loss terms (e.g., data, PDE, IC, BC) present in a PINN [4], the impact of learning biases [5], and sensitivity to initialization [6] and a consequent inability to escape spurious local minima [7–9].

Evolutionary algorithms are a subset of artificial intelligence algorithms that are commonly used to approximate solutions to nonconvex optimization problems with multiple local optima. By using a population-based approach and applying evolutionary principles, evolutionary algorithms can explore the space of possible solutions and find the configuration that provides a balance between accuracy and physical fidelity. This can be especially useful when dealing with complex or nonlinear systems, where traditional gradient descent optimization methods may not be effective. In the context of PINNs, evolutionary algorithms can be used to find a near optimal configuration of the network's parameters in order to more accurately model a given physical system [10], and may present certain advantages over conventional gradient descent methodologies in view of their complicated optimization landscapes [11]. However, despite the potential benefits of using evolutionary algorithms for training PINNs, there has been relatively little research in this area due to the computational challenge of sampling and evaluating populations of solutions in evolutionary algorithms.

Running the algorithm for a large number of iterations or on a large number of training examples can be time-consuming and require significant computational resources. This can sometimes make evolutionary algorithms less practical, or may require the use of specialized hardware such as GPUs or TPUs to run efficiently. Additionally, the computational cost of evolutionary algorithms can increase as the size and complexity of the optimization problem grows, which can constrain applicability on larger, more complex problems.

Despite these challenges, recent developments such as EvoJAX have greatly improved the competitiveness of evolutionary algorithms for training neural networks. EvoJAX is a neuroevolutionary toolkit to train neural networks in a scalable way on hardware accelerators like GPUs and TPUs. The toolkit is built on the JAX framework and uses NumPy for high-performance computations, which are compiled just-in-time to run on the accelerators [12]. This allows EvoJAX to significantly speed up training time by 10-20 times for evolutionary computation experiments [13]. In addition, the availability of a diverse range of evolutionary algorithms on EvoJAX enhances its appeal as a tool for training neural networks [14]. By providing users with a range of options to choose from, EvoJAX allows one to select and modify the algorithm that is most appropriate for the problem at hand. New algorithms can also be designed and implemented on EvoJAX in a reasonably straightforward manner, thus holding the potential of substantially improving the performance and effectiveness of the neuroevolutionary training of PINNs.

To this end, the present work provides a set of five benchmark problems, with associated performance metric and baseline results, to support the development of evolutionary algorithms as an alternative route for enhanced PINN training. As a baseline, we evaluate the performance and speed of using evolutionary algorithms for solving PINNs, specifically the widely adopted Covariance Matrix Adaptation Evolution Strategy (CMA-ES) [15]. The loss and training time of CMA-ES run on JAX, CMA-ES run on TensorFlow (with and without GPU acceleration) [16], and stochastic gradient descent (SGD) run on JAX are provided for the aforementioned five benchmark problems. We provide JAX and TensorFlow implementations of all benchmark problems, and analytical and simulation solutions as supplementary material in the following link <https://github.com/nicholassung97/Neuroevolution-of-PINNs>. By comparing the results of these algorithms on these benchmark problems, we can assess the relative effectiveness and efficiency when using either evolutionary algorithms or stochastic gradient descent for solving

PINNs. These results also provide a common baseline for development and comparison of other optimization algorithms.

## 2. Optimization Algorithms and Deep Learning Frameworks

The aim of this study is to provide baseline performance metrics when using CMA-ES and SGD for solving PINNs. Two commonly used backend implementations (JAX and TensorFlow) are used to build the PINN models, and their relative performances are also compared for the same baseline algorithm (CMA-ES). For the sake of consistency across comparisons, all results are obtained from runs on a workstation with an Intel Xeon W-2275 Processor (19.25M Cache, 3.30 GHz, 14 cores) CPU and two NVIDIA GeForce RTX 3090 GPUs.

Table I summarises the various combinations of PINN optimization algorithms and deep learning framework compared in this report. These combinations have been selected to illustrate i) the acceleration of JAX relative to TensorFlow implementations (with and without GPU acceleration); ii) the performance and training time metrics when using CMA-ES and SGD on the JAX platform (with GPU acceleration) for training PINNs.

Table I: Summary of optimization methods used in current study.

Method	Optimization algorithm		Deep learning framework		GPU-acceleration
	CMA-ES	SGD	JAX	TensorFlow	
1	√			√	
2	√			√	√
3	√		√		√
4		√	√		√

### 2.1. Optimization Algorithms

In this report, we consider using the Covariance Matrix Adaptation Evolution Strategy (CMA-ES) to train PINNs. CMA-ES is a population-based, gradient free optimization algorithm that can be used to approach the global minimum of any complex objective function defined on a continuous search space. It does not require the calculation of exact gradients or other derivatives of the objective function, and instead uses a probabilistic model-based search strategy to sample and explore the space of possible solutions, gradually converging towards a region where the global minimum is likely to be located.

The key feature of CMA-ES is its ability to adapt the search strategy based on the behaviour of the objective function gleaned from the sampled solutions. As an instantiation of an information-geometric optimization procedure, CMA-ES iteratively updates an estimate of the mean and the covariance matrix of a multivariate Gaussian distribution model from which subsequent candidate solutions are to be sampled and evaluated against the objective function. The spread of the solutions allows the algorithm to more effectively explore the space of possible solutions, thereby avoiding the propensity of (point-based) optimization techniques to get stuck in local minima. This adaptive search strategy makes CMA-ES particularly well-suited for complex optimization problems with multiple local optima, such as those encountered in deep learning with nonconvex loss functions. Its well-established performance across many domains motivates the choice of CMA-ES as a competitive baseline evolutionary algorithm for study in this work.

Results from CMA-ES are compared against stochastic gradient descent (SGD), a hugely popular point-based optimization algorithm used to train deep learning models (especially deep neural networks). SGD iteratively updates the model’s parameters in the direction of the negative gradient of the objective function. However, unlike classical gradient descent, SGD uses a stochastic approach, which means that it estimates the gradient of the objective function using a small, randomly selected subset of the training data, rather than the entire dataset. The stochastic update is therefore equivalent to the full gradient in expectation. This makes SGD scalable while

preserving certain advantages of classical gradient descent, thus motivating its widespread use in training large, differentiable models on large datasets.

## 2.2. Deep Learning Frameworks

Both JAX and TensorFlow are popular libraries for deep learning research and development. They provide tools and APIs for implementing and training deep learning models, such as neural networks. Both libraries allow users to define, train, and run deep learning models, and both can be run on a wide range of hardware platforms, including CPUs, GPUs, and TPUs. However, there are some key differences between the two libraries that make JAX generally faster and more efficient than TensorFlow [12].

One major difference is the way JAX and TensorFlow handle automatic differentiation. JAX uses the autodiff system, Autograd, to automatically compute gradients of functions, while TensorFlow uses a static graph representation and reverse-mode automatic differentiation to compute gradients. This means that JAX is able to differentiate functions that are defined dynamically at runtime, while TensorFlow requires the gradient computation to be specified in advance, as part of the model's computational graph.

Another key difference is the implementation of JAX and TensorFlow. JAX uses just-in-time (JIT) compilation to optimize code for specific hardware, allowing it to run operations on CPU, GPU, or TPU without the need to change the code. This makes JAX more flexible and efficient than TensorFlow. Additionally, JAX uses XLA, a domain-specific compiler, to further optimize the performance of deep learning algorithms. This allows JAX to run operations faster than TensorFlow, which uses a more general-purpose compiler.

Given these differences, we will validate the performance of JAX and TensorFlow by comparing their relative performances for the same baseline algorithm (CMA-ES).

## 3. Benchmark Problems

In this study, we use five benchmark problems for PINNs which are representative of real-world phenomena. In particular, these set of benchmark problems were chosen to be diverse in type and application, comprising both ordinary and partial differential equations that describe phenomena in classical mechanics, heat and mass transfer, fluid dynamics and wave propagation (e.g., in acoustics):

1. **Steady state convection-diffusion equation** is an ordinary differential equation that describes the final distribution of a scalar quantity, such as heat or mass, in one spatial dimension in the presence of both convective transport and diffusion. It is commonly used to model transport phenomena in engineering and scientific applications. Using this equation, we simulate the temperature in a spatial domain.
2. **Projectile motion equation** is an ordinary differential equation that governs the motion of an object in a horizontal plane under the influence of gravity  $g$ . The motion of the object is described by the laws of classical mechanics and can be modelled using equations of motion. Using this equation, we simulate the projectile motion of an object released with a pre-determined initial velocity and angle of attack assuming that there is no drag and a hypothetical  $g \approx 3.7$  (e.g., on Mars).
3. **The Korteweg-De Vries (KdV) equation** is a partial differential equation that describes the behaviour of weakly nonlinear, dispersive waves, such as those that occur in shallow water or plasmas. The KdV equation is a simple but powerful model that captures the essential physics of these wave phenomena and has been widely used in a variety of applications, including fluid mechanics, plasma physics, and nonlinear optics. Using this equation, we simulate the collision of two waves of different magnitudes traveling from different locations.
4. **The linearized Burgers' equation** is a partial differential equation that describes the behaviour of viscous, inviscid flow in one spatial dimension. It is a simplified version of the more general Burgers' equation, which is used to model the behaviour of fluid flow in the presence of shock waves and other

complex phenomena. Using this equation, we simulate the propagation of a single waveform at constant velocity.

5. **The non-linear Burgers' equation** is a partial differential equation that describes the behaviour of viscous, inviscid flow in one spatial dimension. It is a more complex and realistic model than the linear Burgers' equation and is used to study the behaviour of fluid flow in the presence of shock waves and other complex phenomena. Using this equation, we simulate the propagation of a single waveform leading to the formation of shock front.

The detailed definitions of these benchmark problems are summarised in Table II.

Table II: Detailed definitions of benchmark problems.

Problem	Physics / differential equation	Initial condition / boundary condition	Computational domain
1) Convection-diffusion	$vu_x - ku_{xx} = 0$ $v = 6, k = 1$	$u(x = 0) = 0$ $u(x = 1) = 1$	$x \in [0, 1]$
2) Projectile motion	$x_{tt} = 0$ $y_{tt} + g = 0$ $g = 3.7$	(Initial displacement): $x(t = 0) = 0$ $y(t = 0) = 2$ (Initial velocity): $x_t(t = 0) = V_o \cos\left(\frac{\alpha_o \pi}{180}\right)$ $y_t(t = 0) = V_o \sin\left(\frac{\alpha_o \pi}{180}\right)$ $V_o = 10, \alpha_o = 80^\circ$	$t \in [0, 2]$
3) Korteweg-De Vries (KdV)	$u_t + v_1 uu_x + v_2 u_{xxx} = 0$ $v_1 = 1, v_2 = 0.001$	$u(x, t = 0) = \frac{3c_1}{(\cosh(a_1(x - x_1)))^2} + \frac{3c_2}{(\cosh(a_2(x - x_2)))^2}$ $a_1 = \frac{1}{2} \sqrt{\frac{c_1}{v_2}}, a_2 = \frac{1}{2} \sqrt{\frac{c_2}{v_2}}$ $c_1 = 0.3, c_2 = 0.1$ $x_1 = 0.4, x_2 = 0.8$	$x \in [0, 1.5]$ $t \in [0, 2]$
4) Linearized Burgers	$u_t + v_1 u_x - v_2 u_{xx} = 0$ $v_1 = 1, v_2 = 0.02$	$u(x, t = 0) = me^{-(kx)^2}$ $k = 2, m = 10$	$x \in [-1.5, 6.5]$ $t \in [0, 2]$
5) Non-linear Burgers	$u_t + uu_x - v_1 u_{xx} = 0$ $v_1 = 0.001$	$u(x, t = 0) = me^{-(kx)^2}$ $k = 2, m = 1$	$x \in [-2, 2]$ $t \in [0, 2]$

## 4. Performance Metrics

Three performance metrics were used to evaluate the effectiveness and efficiency of the optimization methods: training time, training loss, and prediction MSE.

### 4.1. Training Time

Training time is the amount of time it takes for the optimization method to train the PINN model. There are several factors that can affect the training time of the PINN model, including the sample size of the training data, the complexity of the physical laws being modelled, the number of network parameters, and the computational resources available for training. Detailed descriptions of these factors are provided in subsequent sections to facilitate comparison across different optimization methods.

### 4.2. Training Loss

Training loss is a measure of the difference between the predictions made by the PINNs and the known physical laws governing the system being modelled during training. It is calculated by summing the difference between the predicted outputs and the true values at the initial and boundary conditions, as well as the residual of the partial differential equation (PDE) representing the physical laws as shown in Equation 1 where the weights of the loss terms, or the relative importance of each term in the loss function is kept equal at one. This difference, or violation from the governing physics, is quantified using a loss function ( $\mathcal{L}_{Physics}$ ) as summarised in Table III for each benchmark problem. The training loss is used to evaluate the network's performance during the training process. The goal of each optimization method is to train the PINN models to minimize the training loss, such that the PINNs' predictions are as close as possible to the true physical system.

Table III: Loss formulation for benchmark problems.

Problem	Training loss
1) Convection-diffusion	$\mathcal{L}_{Physics} = \mathcal{L}_{PDE} + \mathcal{L}_{BC}$ $\mathcal{L}_{PDE} = \frac{1}{n} \sum_x (v\hat{u}_x(x) - k\hat{u}_{xx}(x))^2$ $\mathcal{L}_{BC} = \frac{1}{2} [(u(x=0) - \hat{u}(x=0))^2 + (u(x=1) - \hat{u}(x=0))^2]$
2) Projectile motion	$\mathcal{L}_{Physics} = \mathcal{L}_{PDE_1} + \mathcal{L}_{PDE_2} + \mathcal{L}_{IC_1} + \mathcal{L}_{IC_2} + \mathcal{L}_{IC_3} + \mathcal{L}_{IC_4}$ $\mathcal{L}_{PDE_1} = \frac{1}{n} \sum_t (\hat{x}_{tt}(t))^2$ $\mathcal{L}_{PDE_2} = \frac{1}{n} \sum_t (\hat{y}_{tt}(t) + g)^2$ $\mathcal{L}_{IC_1} = (x(t=0) - \hat{x}(t=0))^2$ $\mathcal{L}_{IC_2} = (y(t=0) - \hat{y}(t=0))^2$ $\mathcal{L}_{IC_3} = (x_t(t=0) - \hat{x}_t(t=0))^2$ $\mathcal{L}_{IC_4} = (y_t(t=0) - \hat{y}_t(t=0))^2$
3) Korteweg–De Vries (KdV)	$\mathcal{L}_{Physics} = \mathcal{L}_{PDE} + \mathcal{L}_{IC}$ $\mathcal{L}_{PDE} = \frac{1}{n} \sum_{x,t} (\hat{u}_t(x,t) + v_1\hat{u}(x,t)\hat{u}_x(x,t) + v_2\hat{u}_{xxx}(x,t))^2$ $\mathcal{L}_{IC} = \frac{1}{n_x _{t=0}} \sum_{x _{t=0}} (u(x,t=0) - \hat{u}(x,t=0))^2$
4) Linearized Burgers	$\mathcal{L}_{Physics} = \mathcal{L}_{PDE} + \mathcal{L}_{IC}$ $\mathcal{L}_{PDE} = \frac{1}{n} \sum_{x,t} (\hat{u}_t(x,t) + v_1\hat{u}_x(x,t) - v_2\hat{u}_{xx}(x,t))^2$ $\mathcal{L}_{IC} = \frac{1}{n_x _{t=0}} \sum_{x _{t=0}} (u(x,t=0) - \hat{u}(x,t=0))^2$
5) Non-linear Burgers	$\mathcal{L}_{Physics} = \mathcal{L}_{PDE} + \mathcal{L}_{IC}$ $\mathcal{L}_{PDE} = \frac{1}{n} \sum_{x,t} (\hat{u}_t(x,t) + \hat{u}(x,t)\hat{u}_x(x,t) - v_1\hat{u}_{xx}(x,t))^2$ $\mathcal{L}_{IC} = \frac{1}{n_x _{t=0}} \sum_{x _{t=0}} (u(x,t=0) - \hat{u}(x,t=0))^2$

#### 4.3. Prediction Mean Squared Error

The prediction mean squared error (MSE) refers to the error between the predicted solution and the ground truth solution. It is calculated by taking the average of the squared difference between the model's predictions and the true target values. The prediction MSE is important because it provides validation of the model's performance that is independent of the training loss.

To calculate the prediction MSE, we need to have access to the ground truth solution for each benchmark problem. For the convection-diffusion and the projectile motion problems, the ground truth solution can be found analytically. In contrast, the ground truth solution for the Korteweg-De Vries (KdV), the linearized Burgers, and the non-linear Burgers' problems are obtained by utilizing a finite volume scheme for spatial terms, while the temporal terms are integrated by second order Runge-Kutta method. To ensure the convective stability, the convection terms are approximated by second order dispersion-relation preserving finite volume scheme [17], together with universal limiter [18]. The remaining spatial terms are approximated by central difference scheme.

A lower prediction MSE against the ground truth solution indicates better performance of the optimization method in training the PINN model.

## 5. Experimental Study

This section presents results from using evolutionary algorithms to solve the five benchmark problems. These results indicate that evolutionary algorithms, specifically CMA-ES, can be effective at solving PINN problems, even as compared to state-of-the-art SGD methods.

### 5.1. Configurations of PINNs and Optimization Algorithms

A preliminary investigation was conducted to explore the relationship between neural network size and model performance by varying the number of neurons in the hidden layers. An adequate neural network size was selected for each problem to ensure good approximations of the solutions to the differential equations. Additionally, we carried out a hyperparameter search to identify the best optimization settings for both CMA-ES and SGD. For CMA-ES, we tested a range of population sizes (20, 50, 80, 100) and initial standard deviations of the Gaussian distribution model (0.001, 0.005, 0.01, 0.05, 0.1, 0.5). For SGD, we tested a range of learning rates (0.001, 0.005, 0.01, 0.05, 0.1, 0.5). The configurations of the physics-informed neural networks and best settings for both optimization algorithms used for each benchmark problem can be found in Table IV.

Table IV: Configurations of PINNs and optimization algorithms.

Problem	PINN architecture*	Loss evaluation: no. collocation points (IC/BC points)	CMA-ES population size & initial standard deviation	SGD learning rate
1) Convection-diffusion	$(x) - 10 - 10 - 10 - (\hat{u})$ <i>no. network weights = 250</i>	10,000 (2)	80, 5e-2	1e-3
2) Projectile motion	$(t) - 8 - 8 < \begin{matrix} 8 - (\hat{x}) \\ 8 - (\hat{y}) \end{matrix}$ <i>no. network weights = 240</i>	10,000 (1)	80, 1e-3	1e-3
3) Korteweg-De Vries (KdV)	$\begin{matrix} (x) \\ (t) \end{matrix} > 8 - 8 - 8 - 8 - 8 - (\hat{u})$ <i>no. network weights = 240</i>	15,477 (77)	50, 5e-2	1e-1
4) Linearized Burgers	$\begin{matrix} (x) \\ (t) \end{matrix} > 10 - 10 - 10 - (\hat{u})$ <i>no. network weights = 260</i>	51,657 (257)	50, 1e-2	1e-2
5) Non-linear Burgers	$\begin{matrix} (x) \\ (t) \end{matrix} > 8 - 8 - 8 - (\hat{u})$ <i>no. network weights = 176</i>	25,929 (129)	100, 1e-2	1e-1

\*For the PINN architecture, the numbers in between input and output represent the number of nodes in hidden layers. For example,  $(x) - 10 - 10 - 10 - (\hat{u})$  indicates a neural network with single input  $x$ , followed by 3 hidden layers with 10 nodes in each layer, and a single output  $\hat{u}$ . All hidden layers, except the final hidden layer, include a bias term and use *tanh* activation function. The final hidden layer uses *linear* activation function and does not include a bias term.

## 5.2. Baseline Results

In this study, five independent runs of each of the optimization methods were performed and the convergence trends were plotted across time to 180s (Figure 1). The bold lines on the plot represent the mean convergence path, and the shaded areas indicate the range of values from the minimum to the maximum convergence path across the five runs. These results provide interesting insights into the convergence behaviours of the optimization algorithms, which will be discussed in more detail in section 5.2.1 and 5.2.2.

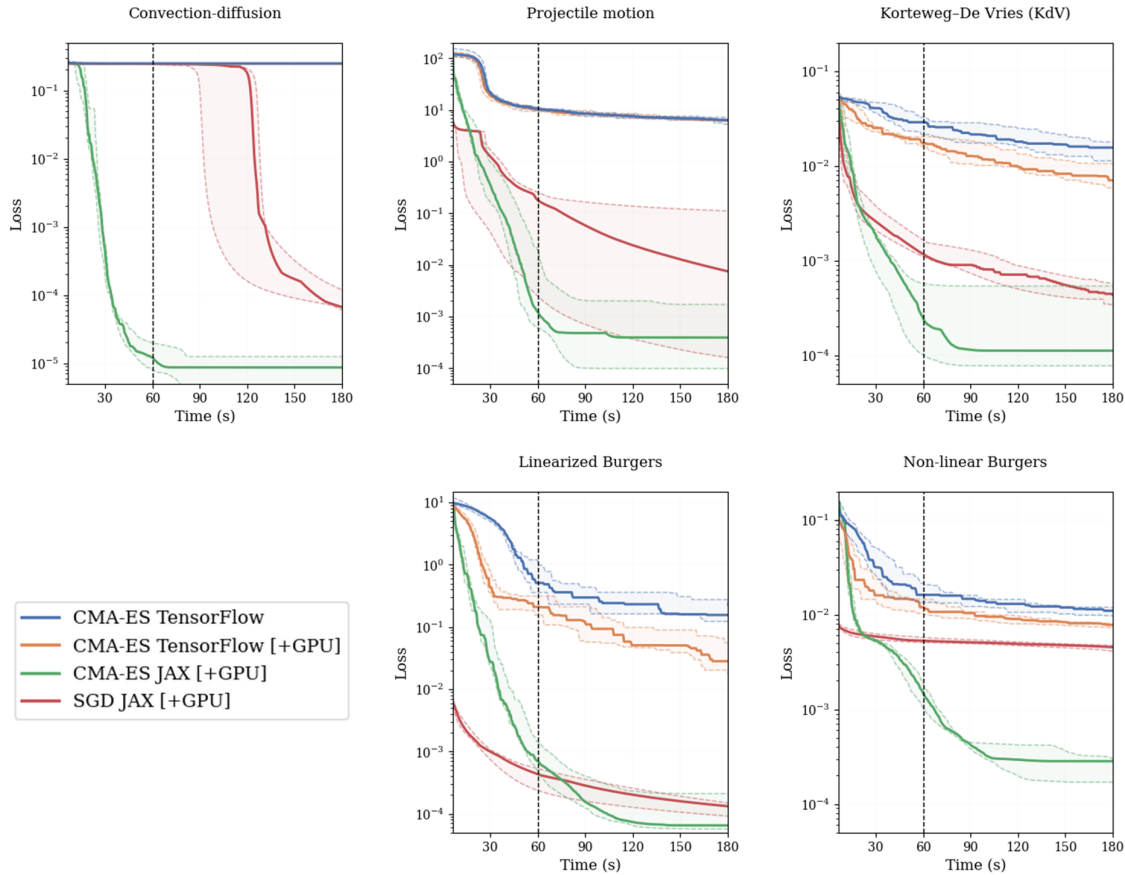


Figure 1: Loss convergence plots.

### 5.2.1. CMA-ES JAX vs CMA-ES TensorFlow

The differences in performance between the CMA-ES implementations on JAX and TensorFlow with GPU acceleration are particularly evident in the loss convergence plot (Figure 1) for the convection-diffusion equation. The CMA-ES implementation on JAX is able to converge much faster than the TensorFlow implementation even with GPU acceleration. In fact, the TensorFlow implementation takes longer than 180s to converge, with the loss beginning to drop noticeably only much later (beyond the range of the plot). Additionally, Figure 1 also indicates that the use of GPU acceleration may not significantly improve the performance of the TensorFlow implementation of CMA-ES. This also further highlights how the JAX framework is able to better utilize the available hardware out-of-the-box, as compared to the TensorFlow framework, which may require more customization. Since the CMA-ES implementation on JAX is able to converge much faster (in terms of wall-clock time) than the TensorFlow implementation, we further conduct all baseline comparisons with implementations on JAX. Nonetheless, it is important to note that the CMA-ES algorithms implemented on JAX and TensorFlow are from different sources and hence may bear some variation in the implementation of the original algorithm.

### 5.2.2. CMA-ES JAX vs SGD JAX

Figure 1 shows that CMA-ES, when run on JAX, typically converges to the minimum much faster than SGD run on JAX. The plots of loss convergence for both optimizers show that the trends intersect, indicating that the two optimizers perform differently at different stages of the convergence process, hence pointing to possible future hybridizations that leverage the best of both worlds. The results also suggest that SGD typically converges more slowly than CMA-ES. This difference in performance may be due to the fact that CMA-ES is better at solving complex PINNs optimization landscapes with many local optima, as it uses multiple samples (whose spread is determined by the covariance matrix of the underlying Gaussian distribution model) to explore the search space. It can therefore more effectively navigate across a complex landscape with local optima, whereas gradient descent is faced with a more difficult task of finding a continuous path of least resistance across the landscape [7]. In addition, SGD is less effective as it can become biased towards local optima if they exist near its initialization, delaying the onset of convergence (e.g., in the convection-diffusion problem).

In a practical context, it is important that PINN training be completed in a reasonable amount of time. Hence, we further compare the training loss and prediction MSE attained by both optimizers after 60 seconds of training. The best scores are highlighted in bold in Table V.

Table V: Training loss and prediction MSE against ground truth solution at 60 seconds.

Problem	Optimizer (JAX)	Training loss	Prediction MSE
1) Convection-diffusion	CMA-ES	<b>1.00e-5</b>	<b>6.38e-9</b>
	SGD	2.45e-1	1.64e-1
2) Projectile motion	CMA-ES	<b>6.73e-4</b>	<b>3.96e-4</b>
	SGD	1.79e-1	2.91e+0
3) Korteweg-De Vries (KdV)	CMA-ES	<b>1.02e-4</b>	<b>7.57e-5</b>
	SGD	1.20e-3	3.77e-3
4) Linearized Burgers	CMA-ES	1.07e-3	<b>1.27e-4</b>
	SGD	<b>7.09e-4</b>	2.64e-3
5) Non-linear Burgers	CMA-ES	<b>1.22e-3</b>	<b>6.82e-4</b>
	SGD	5.74e-3	7.65e-3

The results show that CMA-ES outperforms SGD for four out of the five benchmark problems. CMA-ES also generates lower prediction MSE for all five benchmark problems. To visualize the results, we plotted the solutions generated by CMA-ES JAX and SGD JAX after 60 seconds of training (Figures 2-6).

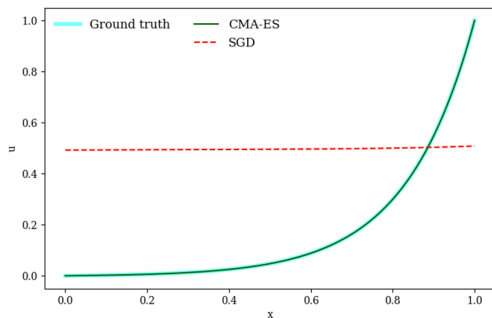


Figure 2. PINN solution for convection-diffusion problem after 60 seconds of training.

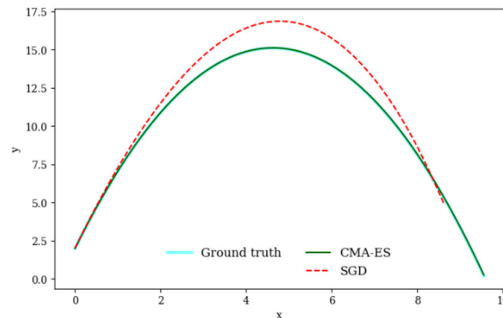


Figure 3. PINN solution for projectile motion problem after 60 seconds of training.

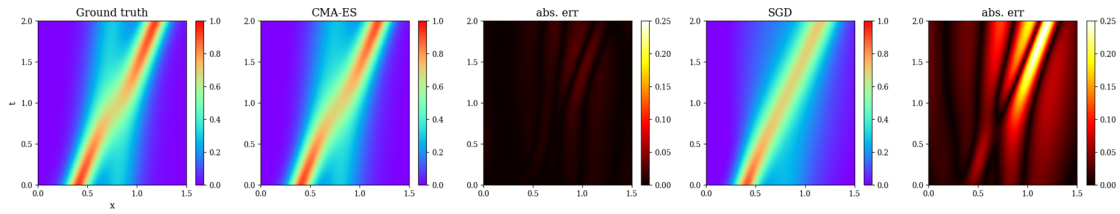


Figure 4. PINN solution for Korteweg–De Vries (KdV) problem *after 60 seconds of training*.

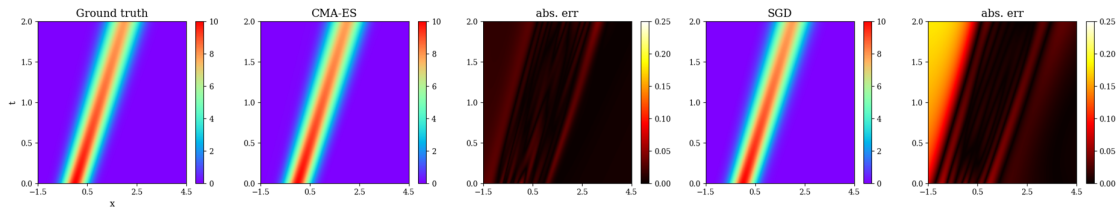


Figure 5. PINN solution for linearized Burgers' problem *after 60 seconds of training*.

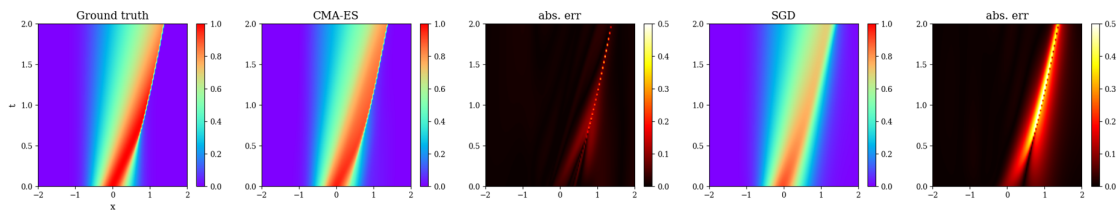


Figure 6. PINN solution for non-linear Burgers' problem *after 60 seconds of training*.

In the linearized Burgers' (Figure 5) problem, the solution generated by both optimizers are visually similar to the simulated solutions. However, for the convection-diffusion (Figure 2), projectile motion (Figure 3), KdV (Figure 4), and non-linear Burgers' (Figure 6) problems, the solution generated by CMA-ES is more similar to the simulated solution compared to the solution generated by SGD, which has a noticeable difference. The absolute error plots in Figures 4, 5 and 6 clearly illustrate the accuracy of the predicted solution, with a smaller error for solutions generated by CMA-ES indicating a better match to the true target solutions.

## 6. Conclusion

This report evaluates the performance of different optimization methods and implementation backends on five PINN benchmark problems. Our results show that evolutionary algorithms, particularly CMA-ES, have the potential to be more effective at solving these problems than the typically-used SGD. It is hoped that this work will further support the exploration and development of alternative optimization algorithms, including evolutionary algorithms, for the complex task of optimizing PINNs, thereby further advancing the possibilities of PINN models for other complex, real-world engineering problems and challenges.

## Reference

- [1] M. Raissi, P. Perdikaris, G.E. Karniadakis, Physics-informed neural networks: A deep learning framework for solving forward and inverse problems involving nonlinear partial differential equations, *J Comput Phys.* 378 (2019) 686–707. <https://doi.org/10.1016/J.JCP.2018.10.045>.
- [2] G.E. Karniadakis, I.G. Kevrekidis, L. Lu, P. Perdikaris, S. Wang, L. Yang, Physics-informed machine learning, *Nature Reviews Physics* 2021 3:6. 3 (2021) 422–440. <https://doi.org/10.1038/s42254-021-00314-5>.
- [3] A.S. Krishnapriyan, A. Gholami, S. Zhe, R.M. Kirby, M.W. Mahoney, Characterizing possible failure modes in physics-informed neural networks, *Adv Neural Inf Process Syst.* 32 (2021) 26548–26560. <https://doi.org/10.48550/arxiv.2109.01050>.

- [4] T. de Wolff, H.C. Lincopi, L. Martí, N. Sanchez-Pi, MOPINNs: An Evolutionary Multi-Objective Approach to Physics-Informed Neural Networks, *GECCO 2022 Companion - Proceedings of the 2022 Genetic and Evolutionary Computation Conference*. (2022) 228–231. <https://doi.org/10.1145/3520304.3529071>.
- [5] N. Rahaman, A. Baratin, D. Arpit, F. Draxler, M. Lin, F.A. Hamprecht, Y. Bengio, A. Courville, On the Spectral Bias of Neural Networks, *36th International Conference on Machine Learning, ICML 2019*. 2019-June (2018) 9230–9239. <https://doi.org/10.48550/arxiv.1806.08734>.
- [6] J. Cheng Wong, C. Ooi, A. Gupta, Y.-S. Ong, Learning in Sinusoidal Spaces with Physics-Informed Neural Networks, *IEEE Transactions on Artificial Intelligence*. (2022) 1–15. <https://doi.org/10.1109/TAI.2022.3192362>.
- [7] T. Garipov, P. Izmailov, D. Podoprikin, D. Vetrov, A.G. Wilson, Loss Surfaces, Mode Connectivity, and Fast Ensembling of DNNs, *Adv Neural Inf Process Syst*. 2018-December (2018) 8789–8798. <https://doi.org/10.48550/arxiv.1802.10026>.
- [8] F.M. Rohrhofer, S. Posch, B.C. Geiger, On the Pareto Front of Physics-Informed Neural Networks, (2021). <https://doi.org/10.48550/arxiv.2105.00862>.
- [9] V. Gopakumar, S. Pamela, D. Samaddar, Loss Landscape Engineering via Data Regulation on PINNs, (2022). <https://doi.org/10.48550/arxiv.2205.07843>.
- [10] K.O. Stanley, J. Clune, J. Lehman, R. Miikkulainen, Designing neural networks through neuroevolution, *Nature Machine Intelligence* 2019 1:1. 1 (2019) 24–35. <https://doi.org/10.1038/s42256-018-0006-z>.
- [11] J.C. Wong, A. Gupta, Y.-S. Ong, Can Transfer Neuroevolution Tractably Solve Your Differential Equations?, *IEEE Comput Intell Mag*. 16 (2021) 14–30. <https://doi.org/10.1109/MCI.2021.3061854>.
- [12] J. Bradbury, R. Frostig, P. Hawkins, M.J. Johnson, C. Leary, D. Maclaurin, G. Necula, A. Paszke, J. VanderPlas, S. Wanderman-Milne, Q. Zhang, JAX: composable transformations of Python+NumPy programs, (2018). <http://github.com/google/jax>.
- [13] Y. Tang, Y. Tian, D. Ha, EvoJAX: Hardware-Accelerated Neuroevolution, *GECCO 2022 Companion - Proceedings of the 2022 Genetic and Evolutionary Computation Conference*. (2022) 308–311. <https://doi.org/10.1145/3520304.3528770>.
- [14] R.T. Lange, evosax: JAX-based Evolution Strategies, (2022). <http://arxiv.org/abs/2212.04180> (accessed December 14, 2022).
- [15] N. Hansen, The CMA Evolution Strategy: A Comparing Review, *Towards a New Evolutionary Computation*. (2006) 75–102. [https://doi.org/10.1007/3-540-32494-1\\_4](https://doi.org/10.1007/3-540-32494-1_4).
- [16] M. Abadi, A. Agarwal, P. Barham, E. Brevdo, Z. Chen, C. Citro, G.S. Corrado, A. Davis, J. Dean, M. Devin, S. Ghemawat, I. Goodfellow, A. Harp, G. Irving, M. Isard, Y. Jia, R. Jozefowicz, L. Kaiser, M. Kudlur, J. Levenberg, D. Mane, R. Monga, S. Moore, D. Murray, C. Olah, M. Schuster, J. Shlens, B. Steiner, I. Sutskever, K. Talwar, P. Tucker, V. Vanhoucke, V. Vasudevan, F. Viegas, O. Vinyals, P. Warden, M. Wattenberg, M. Wicke, Y. Yu, X. Zheng, TensorFlow: Large-Scale Machine Learning on Heterogeneous Distributed Systems, (2016). <https://doi.org/10.48550/arxiv.1603.04467>.
- [17] P.H. Chiu, An improved divergence-free-condition compensated method for solving incompressible flows on collocated grids, *Comput Fluids*. 162 (2018) 39–54. <https://doi.org/10.1016/j.compfluid.2017.12.005>.
- [18] B.P. Leonard, The ULTIMATE conservative difference scheme applied to unsteady one-dimensional advection, *Comput Methods Appl Mech Eng*. 88 (1991) 17–74. [https://doi.org/10.1016/0045-7825\(91\)90232-U](https://doi.org/10.1016/0045-7825(91)90232-U).